Vol. 15: 145–159, 2023
https://doi.org/10.3354/aei00458

AQUACULTURE ENVIRONMENT INTERACTIONS
Aquacult Environ Interact

Published June 1



# Spatio-temporal analysis of sediment plumes formed by mussel fisheries and aquaculture in the western Wadden Sea

**H. M. Jansen[1,2,*], L. van den Bogaart[1], A. Hommersom[3], J. J. Capelle[1]**

[1]Wageningen Marine Research, Korringaweg 7, 4401 NT Yerseke, The Netherlands
[2]Aquaculture and Fisheries Group, Wageningen University, De Elst 1, 6708 WD Wageningen, The Netherlands
[3]Water Insight, Fahrenheitstraat 42, 6716 BR Ede, The Netherlands

ABSTRACT: The Wadden Sea is a highly dynamic tidal system and an important area for a variety of species, including wild and cultivated mussels. Increased suspended sediment concentrations may negatively affect ecosystem functioning across trophic levels; hence, insight into the effects of anthropogenic activities is of importance. The aim of this study was to investigate the scale of sediment resuspension associated with commercial mussel cultivation activities. Turbidity prior to and during fisheries and harvest was investigated by *in situ* measurements with towed and fixed sensors. Four case studies were selected to represent maximum disturbance. For one case study, sediment resuspension was further investigated by analysis of satellite images. The *in situ* measurements showed that turbidity is enhanced by mussel fisheries and harvest but that effects are limited in time and space. Turbidity enhancement during fisheries was several-fold higher than that during harvest, whereas the spatial scale of both activities was limited to their direct vicinity. In contrast to the *in situ* study, the satellite image analysis identified a spatial magnitude that extended over a somewhat larger spatial scale, in the form of a dark water plume, and further revealed that this plume consisted of high concentrations of coloured dissolved organic matter (CDOM), rather than suspended particles. Along with turbidity, CDOM thus seems an important consideration for determining light attenuation in a water body affected by anthropogenic seafloor disturbance. As we presented case studies that were expected to represent maximum impact, we conclude that there is no specific need for further in-depth studies that allow upscaling to ecosystem-wide effects.

KEY WORDS: Aquaculture · Shellfish · Environmental impact · Turbidity · Coloured dissolved organic matter · CDOM · Satellite · *In situ*

## 1. INTRODUCTION

The Wadden Sea is an important coastal wetland and one of the largest uninterrupted intertidal ecosystems worldwide (Lotze 2007, Elias et al. 2012). It is a highly dynamic system, in which large amounts of sediments are regularly transported (De Jonge 1992, Austen et al. 1999, Elias et al. 2012, Van Duren et al. 2015). Since construction of the Afsluitdijk in 1932, closing off the Wadden Sea from the former Zuider Sea (currently Lake IJssel), the Wadden Sea has still not regained morphological equilibrium (Elias et al. 2005, 2012, Vroom et al. 2012). Turbidity in the Wadden Sea is high and variable, and it has been argued that turbidity is increasing (Giesen et al. 1990), but this is debated by others (Philippart et al. 2013). In addition to natural processes, anthropogenic activities like dredging and salt and gas extraction as well as fisheries and shellfish aquaculture contribute to sediment resuspension and transport in the Wadden

*Corresponding author: henrice.jansen@wur.nl



Publisher: Inter-Research · www.int-res.com

Sea system. These activities are known to increase turbidity and sedimentation, but the magnitude and scale of these effects are largely unknown for the Wadden Sea region.

Increased sediment concentrations in the water column have the potential to negatively affect ecosystem functioning through enhanced sedimentation and/or enhanced turbidity (Henley et al. 2000, Kaiser et al. 2006, Airoldi & Beck 2007, Österling et al. 2010). Enhanced sedimentation may lead to smothering of benthic life and changes in sediment characteristics that prevent settlement of new species (Thrush et al. 2004, McLeod et al. 2012). The consequences of enhanced turbidity range from effects on primary producers such as algae and eelgrass as a result of changes in light penetration to adaptation of benthic life and reduced visibility for fish and bird populations (Henley et al. 2000, Duarte 2002, Morrison et al. 2009, Castorani et al. 2015, Figueiredo et al. 2016, Ortega et al. 2020).

Considering these potential negative effects of increased suspended sediment concentrations on ecosystem functioning, it is important to identify the spatio-temporal scale of turbidity enhancement caused by anthropogenic activities. The current study thereby focuses on the sediment dynamics associated with mussel aquaculture in the Wadden Sea. The role of mussel aquaculture in sediment dynamics is 2-fold. On the one hand, mussels continuously filter suspended particulate material from the water column. It is estimated that on an annual basis, 1.2 to 2.4 million t of silt is being captured by mussels in the Wadden Sea (De Groot et al. 2013). This may have a positive impact on the turbidity and visibility of the water column (Cadée & Hegeman 1974, Dankers & Koelemaij 1989, Beukema & Cadée 1996, Hawkins et al. 1996, Schröder et al. 2014), which is also addressed as an ecosystem service provided by bivalves (Cranford 2019). On the other hand, organic-rich sediment that has accumulated within mussel beds or on bottom culture plots is resuspended during fisheries and (post-)harvest activities, which may temporarily enhance turbidity in the water column during and after these activities. The environmental impact of mussel dredging has gained much attention over the past decades. Most research focused on quantifying the direct effects of dredging on bottom fauna (Dolmer et al. 1999, 2001, 2012, Frandsen et al. 2015, Craeymeersch et al. 2023), whereas studies on how sediment resuspension affects water quality are limited. A recent study that evaluated dredging by one mussel vessel in a sheltered estuary in Denmark demonstrated that the turbidity of the water column was most affected by fishing intensity and current speed (measured up to 0.15 m $s^{-1}$) and concluded that the overall spatio-temporal impact of dredging in the study area was considered to be low (Pastor et al. 2020). Current speeds in the Wadden Sea can be up to 10-fold higher (1.5 m $s^{-1}$; McBride et al. 2013), and fishing intensity is also higher (Smaal et al. 2021). The hydrodynamic conditions of an area determine whether ecosystem functioning is primarily affected by sedimentation or by enhanced turbidity (Nieuwaal 2001). In regions of low hydrodynamic energy, settling of suspended sediments has greater effects than light attenuation. In regions of high hydrodynamic energy, the reverse is true, as suspended sediments stay in suspension.

The aim of the current study was to define the (maximum) spatial scale of turbidity enhancement caused by sediment resuspension associated with commercial mussel cultivation activities in a highly dynamic environment. The spatial delineation of an area with enhanced suspended sediment concentrations, measured as turbidity, is also referred to as a sediment plume. As anthropogenic activities that cause seafloor disturbance are expected to affect local turbidity and sedimentation rather than total sediment transport (Van Duren et al. 2015), we aimed to evaluate to what extent mussel culture contributes to local turbidity enhancement in subtidal areas of the western Wadden Sea. Sediment plumes were investigated for 4 case studies using a combination of empirical data collection with turbidity sensors and, when available, analysis of satellite data. The case studies were selected to represent high sediment disturbance, i.e. areas with high fisheries activity or areas where the silt fraction in the sediment is high, and allowed us to investigate the maximum spatial and temporal resolution of the sediment plume created by mussel cultivation in the western Wadden Sea.

## 2. MATERIALS AND METHODS

Sampling campaigns were connected to commercial mussel cultivation (seed fisheries, harvest or post-harvest activities). Mussel aquaculture in the Wadden Sea is characterized by bottom cultivation; mussel seed is either fished from natural beds or collected by suspended longlines (Kamermans & Capelle 2019, Smaal et al. 2021) and subsequently relayed onto bottom plots for further growth to commercial size until harvest. A mussel dredge (Smaal et al. 2021) is used during seed fisheries and harvest of mussels. Post-harvest, the accumulated silt and sediment is removed from the plots by resuspension of

the sediment through intense dredging to start the new cultivation cycle with a clean and homogeneous plot. Both fisheries and cultivation activities exclusively take place in subtidal areas.

### 2.1. Study design

Field measurements to investigate turbidity during fisheries on wild seed beds were carried out at Location I (Omdraai) and II (Breesem) in May 2017 and on commercial bottom plots (post-)harvest at Location III (Inschot) and IV (Oosterom) in November 2017 (Table 1, Fig. 1). Prior to fisheries activities, the contours of seed beds are mapped during a standardised monitoring program that provides input for the annual fishing plans (Troost et al. 2022). Hence, mussel fisheries generally aggregate at specific locations that have been identified as promising in terms of densities and size of mussel seed. In spring, at the time of our sampling campaign, 6 to 10 boats were aggregated at Location I, and 4 to 6 boats were fishing at Location II. The number of boats varied throughout the sampling campaign, as commercial vessels might move between several seed beds during the day. While present, and apart from hauling, all vessels were continuously dredging the seed bed with four 1.9 m wide mussel dredges per vessel. In autumn, field campaigns were performed to investigate sediment dynamics during harvest on bottom plots. Bottom plots are generally situated in shallow gullies (<3 m NAP [Amsterdam Ordnance Datum, reference for sea level]) or alongside deeper gullies (>3 m NAP). The effects of post-harvest sediment removal on suspended sediment dynamics were examined on 1 mussel plot at Location III. The sediment at this site is characterized by a high fraction of silt (Dankers et al. 2006, Dutch Mussel Producers Organisation pers. comm.) and therefore expected to generate high impact on suspended sediments. Location IV consisted of a block of clustered mussel plots where multiple activities occurred during the sampling campaign (both harvest and post-harvest sweeping). A cloud-free Sentinel-2 Multi-Spectral Instrument (MSI) satellite image that corresponded to the period when the field turbidity measurements were carried out was only available for Location IV. This image was used to evaluate the spatial magnitude of the sediment plume and its spectral properties.

### 2.2. Field measurements

At each location, the spatial extent of mussel dredging was determined by measuring turbidity of the water column along different transects during fisheries or harvest activities (Fig. 2). The transects were assigned with the aim of providing a good spatial coverage of the sediment plume as follows: (1) transects starting upstream of the fisheries or harvest zone, crossing this zone and moving downstream along with the current direction; (2) transects perpendicular to the current direction; and (3) alternative transects that depended on morphology of the area. The timing of the sampling campaigns was based on the activities (measurements performed >1 h after fisheries and >30 min after harvest started) and tidal cycle (unidirectional current direction during incoming tides). The main current direction was projected by the tidal cycle, topography of the site, existing maps indicating general current directions and using the experience of local water managers.

Table 1. Characteristics of the 4 case study sites and information on sampling campaigns. Current speed data were obtained from the open-access database GETM (source: https://codm.hzg.de/codm/Formular.jsp#). MLW: mean low water; MHW: mean high water

| Location | Site description | | Sampling characteristics | | | |
|---|---|---|---|---|---|---|
| | Depth in reference to MLW/MHW (cm) | Current speed (m $s^{-1}$) | Date (2017) | Culture activity | No. of commercial vessels | Area fished or harvested (ha) |
| I. Omdraai | −172/−74 | 0–0.5 | 9 May (08:00–10:15 h) | Seed fisheries | 6–10 | 46 |
| II. Breesem | −302/−173 | 0.2–0.4 | 10 May (08:15–10:15 h) | Seed fisheries | 4–6 | 33 |
| III. Inschot | −1074/−665 | 0.4–0.45 | 21 Nov (08:00–09:45 h) | Post-harvest (single plot) | 1 | 3.1 |
| IV. Oosterom | −1488/−173 | 0–0.2 | 7 Nov (10:00–11:30 h) | Harvest and post-harvest (cluster of plots) | 7 | 32.5 |

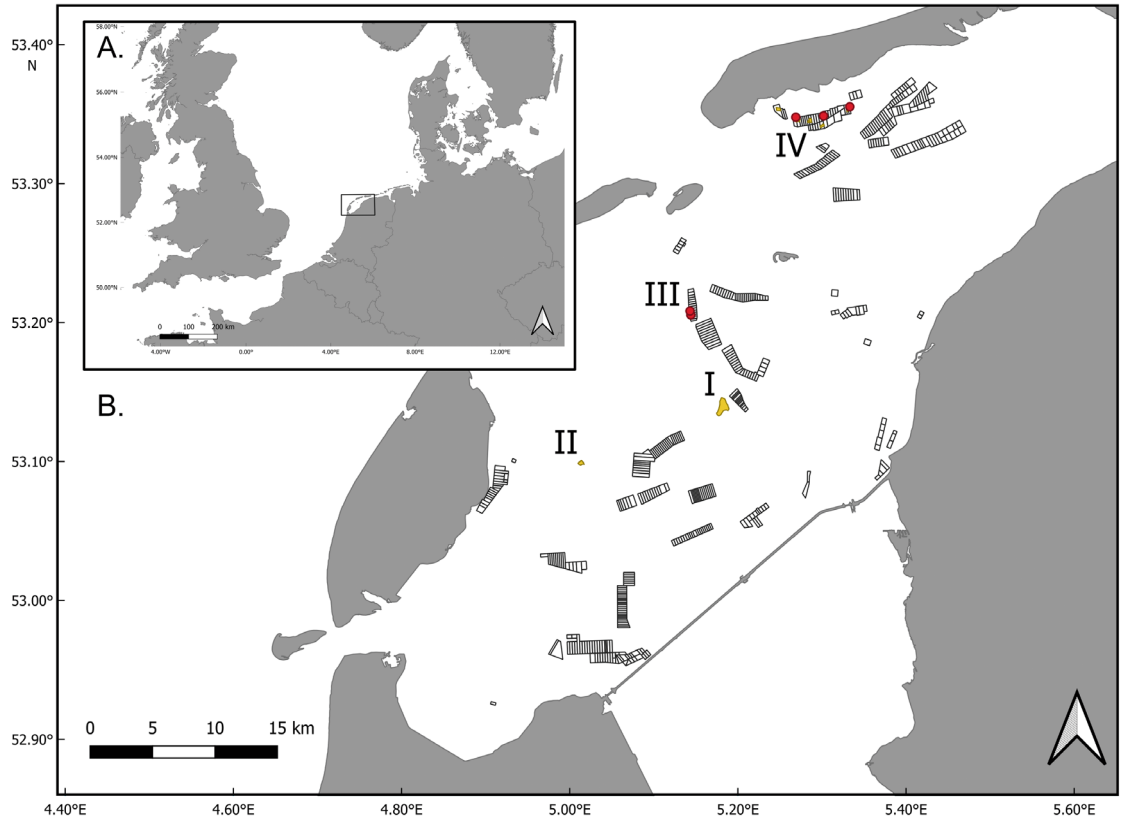


Fig. 1. Western Wadden Sea, indicating study sites (I: Omdraai; II: Breesem; III: Inschot; IV: Oosterom). Black polygons indicate the positions of commercial mussel plots. Red dots refer to the fixed sensors and yellow polygons to fisheries or harvest areas (see also Fig. 2)

Turbidity was logged at 1 s time intervals with a high-resolution turbidity sensor (Infinity-CLW), measuring scattered light and expressing turbidity in the formazin turbidity unit (FTU). The sensor was submerged approximately 1 to 1.5 m below the water surface at the side of the research vessel, well in front of the propeller, where no impact of the engines can be expected. Pilot studies at multiple sites during culture activities investigated turbidity along depth profiles and showed that at this depth, the maximum turbidity is expected. This suggests that turbidity is not only an effect of sediment resuspension by dredging but also originates from water exiting the mussel vessel. Once the sensor was submerged, the boat navigated at a constant slow speed (up to 4 knots) in straight transects through the fisheries or harvest zone. GPS coordinates of each location were noted, as well as start and end times, to calculate distance and to link to the turbidity data logged by the sensors.

Additional to the transects, fixed Infinity turbidity sensors were deployed at Locations III and IV to provide insight into the temporal dynamics of the sediment plume during and after harvest (Fig. 2). At Location III, sensors were deployed at 2 stations for a period of 24 h, 1 on the edge of the mussel plot where maximum impact was expected (downstream during the timeframe when post-harvest activities took place) and 1 at an upstream reference station. These 24 h included periods with and without harvest activities on the plot. At each station, 2 sensors were deployed, 1 at 50 cm above the sediment and 1 approximately around the low water line. At Location IV, 3 sensors were deployed along the block of plots at 50 cm above the sediment.

To correlate the high-resolution turbidity data (FTU) with suspended particulate matter (SPM, mg $l^{-1}$), water samples were collected in triplicate at several (minimum of n = 4 per sampling d) high-, medium- and low-turbidity sites. In the laboratory, samples were filtered according to standard protocols (Grasshoff et al. 1999), using pre-burned and pre-weighed Whatman GF/C filters. After filtration, filters were rinsed with ammonium formate to remove salt particles. Filters were dried for 24 h at 70°C and weighed to define dry weight and subsequently burned at

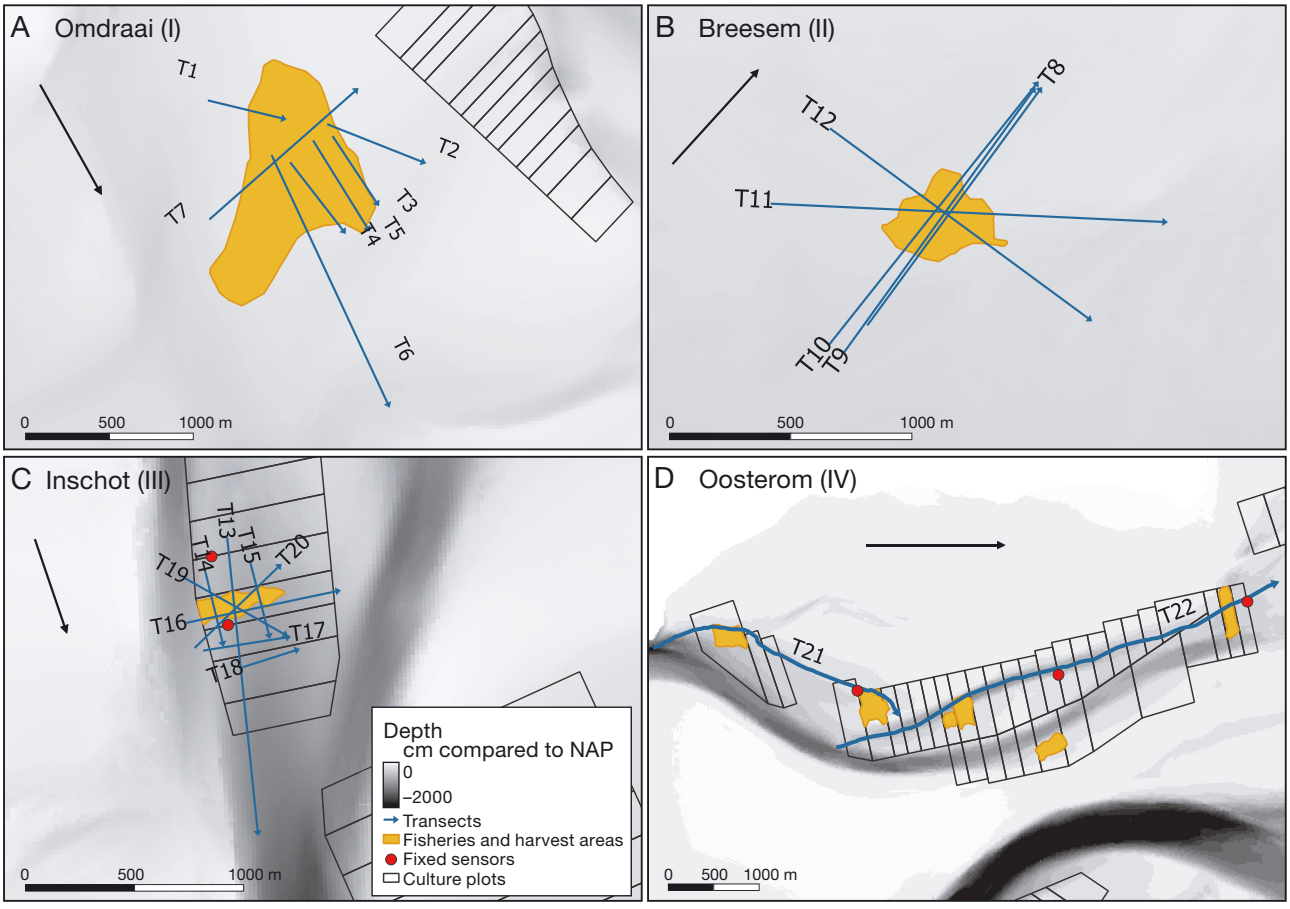


Fig. 2. Location of transects (blue arrows) and (A,B) fisheries and (C,D) harvest areas (yellow contours) during the sampling campaigns. Black box data (GPS positioning system on board commercial fishing vessels) were used to define the fisheries or harvest contours. Projected current direction is indicated by the black arrow, and black polygons present the borders of commercial mussel plots. Red dots indicate the locations where fixed meters were deployed. Depth profiles are projected by the grey gradients. NAP: Amsterdam Ordnance Datum, reference for sea level

450°C for 5 h and weighed to calculate ash-free dry weight and organic fraction. FTU to SPM correlations were analysed by linear regression for spring and autumn sampling campaigns separately because of expected seasonal variations (Jafar-Sidik et al. 2017).

### 2.3. Satellite analysis

Data from the MSI on Sentinel-2 were used for the spectral analysis of the plumes. The amount of light measured by a satellite sensor largely originates from the reflection on atmospheric molecules and only to a small extent from the water because of the strong absorption of water itself. To be able to derive e.g. chlorophyll concentrations, it is standard to apply an atmospheric correction (AC) model. However, AC models for inland and other complex waters are far from perfect (Warren et al. 2019). In the case of the Wadden Sea, with high concentrations of sediments and the presence of tidal flats, application of an AC model is prone to errors. In addition, AC models that are based on neural networks (such as C2RCC; Brockmann et al. 2016) might not be able to provide an appropriate output for a pixel that contains a water colour and that might not have been in its training range. Since the plumes are much darker than most surrounding water pixels, application of an unsuitable AC model might introduce errors. Therefore, the reflectance at the top of the atmosphere (TOA) was used for tracing the plume, while the Rayleigh correction (Ruescas & Müller 2021) was carried out to test the method to detect black sediments as proposed by Vanhellemont & Ruddick (2015). The Rayleigh corrected reflectance (rBRR) is not corrected for aerosol effects and is suitable for comparison of pixels inside and outside a plume.

To determine the spectral properties of the material in the plume, a transect was drawn in the area that intersected non-plume and plume pixels. For each spectral band, a plot was made based on a transect perpendicular to the plume and the transect of the vessel to analyse the variability in the spectral band between plume and non-plume pixels. Additionally, the magic wand tool in the software SNAP was used to identify the plumes with a spectral angle mapper. The tool was used on all 13 spectral bands of the sensor; the setting spectrum transformation was set to identity (instead of integral or derivative), and the spectra were not normalised. The similarity metric was set to distance (instead of average or min-max). A true colour view of the image was used to select 5 pixels that, by eye, belonged to the plume. Then, the tolerance was adjusted up to the point where, by eye, the classification algorithm mapped all pixels belonging to the plumes. The plume shape was used as an overlay in each spectral band (1–8a) for visual inspection and in the analysis of the perpendicular transect plot.

The black sediments approach by Vanhellemont & Ruddick (2015) is designed on Landsat-8 spectral bands and is based on 2 criteria: (1) the near-infrared (NIR) marine reflectance is greater than a threshold for turbid waters (ρw band 5 > 0.01), and (2) the maximum marine reflectance in 3 visible bands (ρw 2, 3 and 4) is low for this turbidity (<0.07). The first criterion removes cases where absorption, in the visible bands, is caused by coloured dissolved organic matter (CDOM) rather than by suspended sediments (Vanhellemont & Ruddick 2015). In this study, the Sentinel-2 bands 2, 3, 4 and 8a are used instead of the Landsat-8 bands, since the spectral ranges are comparable.

## 3. RESULTS

### 3.1. Fisheries activities

At Location I, the vessels clustered densely on one mussel bed, and due to safety reasons, it was impossible to include upstream, fisheries zone and downstream areas during 1 transect. Instead, we started in the middle of all activity and moved downstream (Fig. 3B) and included 1 transect that started upstream and went into the fisheries zone (Fig. 3A). At Location II, up- and downstream areas were included in the same transect that also crossed the fisheries zone (Fig. 3D). Fig. 3 shows that turbidity was strongly enhanced in the (centre of the) fisheries zone but also that the turbidity along the transects was patchy, even within the sites where intensive

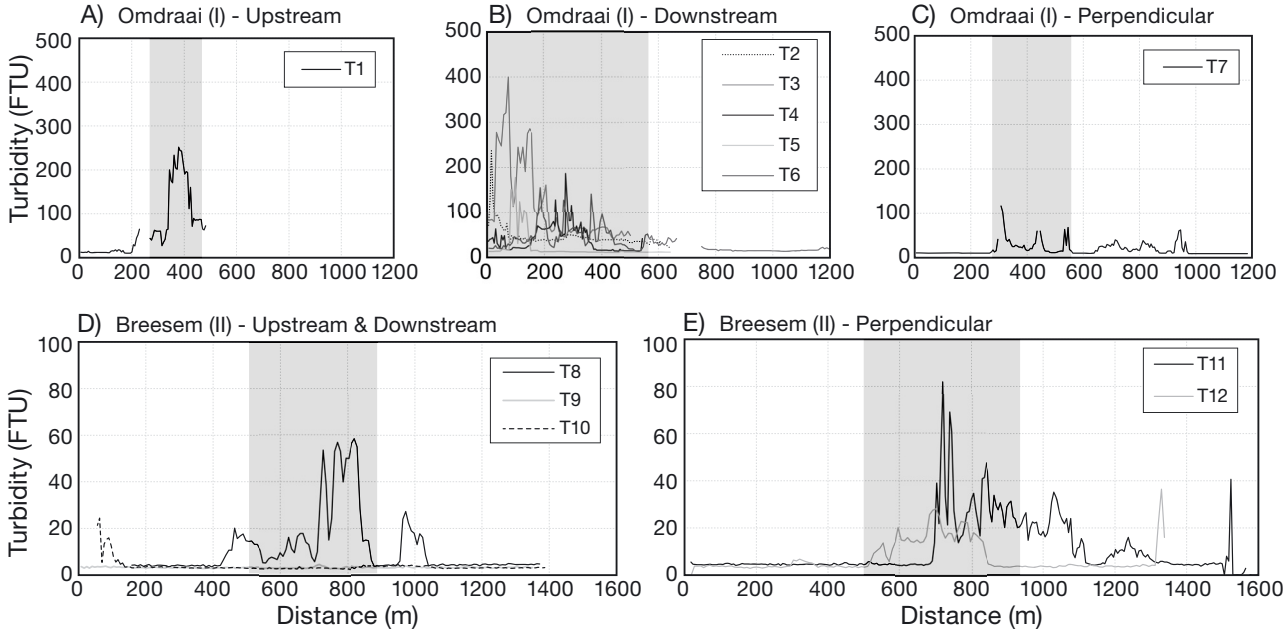


Fig. 3. Turbidity profiles of transects (T) observed during seed fisheries at Locations (A,B,C) I (Omdraai) and (D,E) II (Breesem). Transects in line with the main current direction include upstream, fisheries zone and downstream areas (A,B,D) where the current direction is from left to right. Transects perpendicular to the current direction include the fisheries zone and areas on both sides with no fisheries activity (C,E). Distance on the *x*-axis indicates the length of the transect from the moment the sensor was submerged in the water column. Grey shading indicates the approximate fisheries zone. For position of transects and fisheries zone, see Fig. 2. FTU: formazin turbidity unit

fisheries took place for several hours. This indicates that the sediment plume is heterogeneous and consists of patches that include higher sediment concentrations, which was also visually observed. Due to the observed patchiness along transects, contour plots could not be established, and the exact delineation of the plume area and boundaries could not be defined. The maximum turbidity at Locations I (200–400 FTU) and II (60–80 FTU) was substantially higher than the background turbidity (5–10 FTU) measured at the upstream sections of the transect (Fig. 3). Although turbidity can be high in close proximity to fishing vessels, the sediment concentrations dropped quickly back to near-background levels (Fig. 3B,D).

### 3.2. Harvest and post-harvest activities

Harvest and post-harvest activities at Locations III and IV resulted in turbidity values that were up to 6 times higher on the cultivation plots compared to background values (Fig. 4; Table 1). Background values (~5 FTU) were determined from the upstream sections, as separate reference transects could only be obtained during a different phase of the tidal cycle (data not shown) and resulted in values that were almost double the upstream turbidity values. The up- and downstream transects (T13–T15) at Location III suggest that outside the border of the plot, values were still slightly enhanced (Fig. 4A), which was, however, not confirmed by the perpendicular transects at 100 m (T17) and 200 m (T18) away from the cultivation plot (Fig. 4B). This cultivation plot is situated in a gully, and depth decreases from west to east (see Fig. 2). Higher (background) turbidity values were observed in the shallow areas; see transects T16 (Fig. 4B) and T19–T20 (Fig. 4C). The fixed turbidity sensors at Location III also yielded highly variable but enhanced turbidity concentrations at the time when post-harvest activities took place, while at the same time low and stable turbidity was observed at the reference location (Fig. 5A–C). When post-harvest activities were terminated, turbidity almost directly decreased at the culture plot, and the reference and culture plot were again similar in terms of both temporal patterns and magnitude of turbidity (Fig. 5B,C). The measurements with fixed sensors demonstrated that background values varied depending on the tidal phase, with generally increased values around the moment when the tides were turning.

At Location IV, the transects crossed a number of adjacent mussel plots, and at some plots, harvest or post-harvest activities took place (Fig. 4D,E) and showed that turbidity increased at and right after cul-

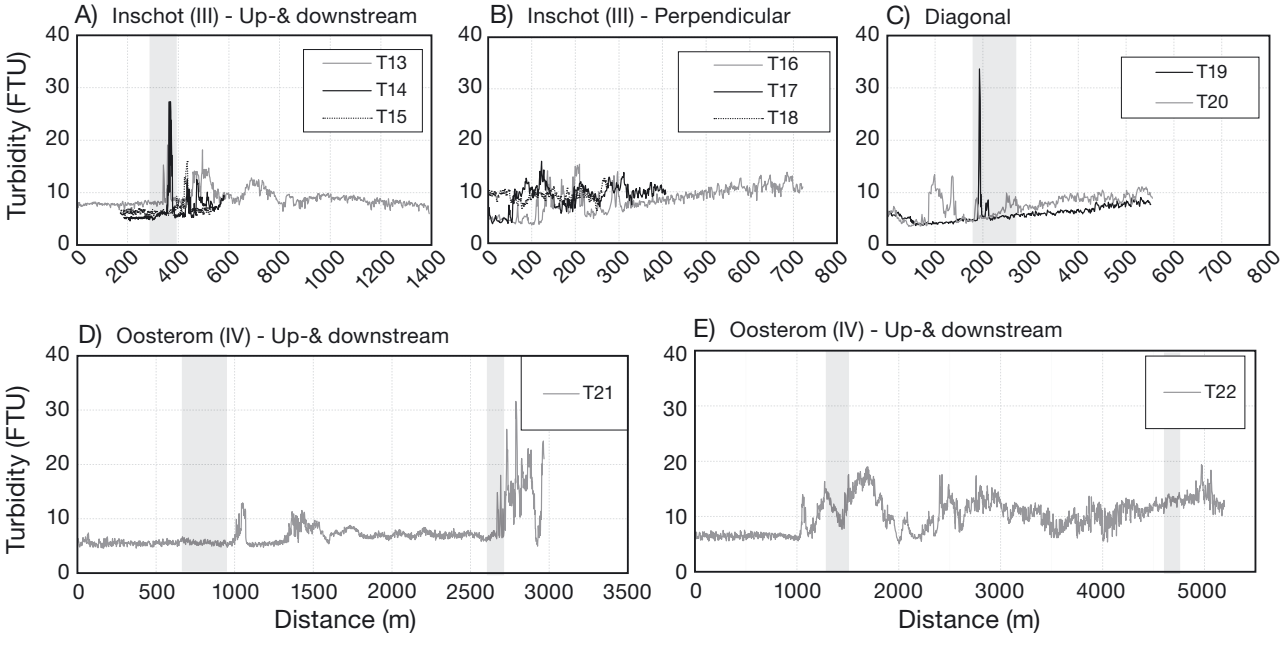


Fig. 4. Turbidity profiles of transects (T) observed during (post) harvest activities at Locations (A,B,C) III (Inschot) and (D,E) IV (Oosterom). Transects in line with the main current direction include upstream, culture plot and downstream areas (A,D,E) where the current direction is from left to right. Transects perpendicular to the current direction (B) and diagonal on the plot (C) include the culture plot and areas on both sides with no fisheries activity. Distance indicates the length of the transect from the moment the sensor was submerged in the water column. Grey shading indicates the approximate harvest zone. For position of transects and fisheries zone, see Fig. 2. FTU: formazin turbidity unit

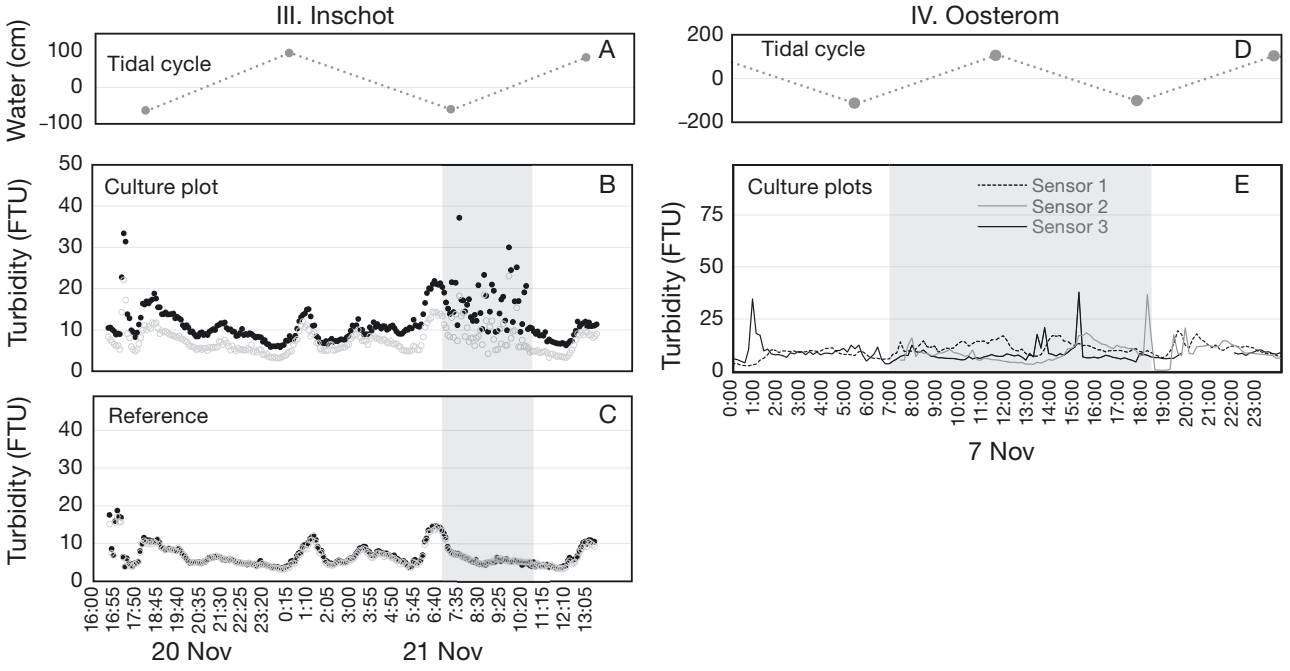


Fig. 5. Turbidity before, during and after (post-) harvest activities. Location III (Inschot; A,B,C) measured with fixed sensors at 50 cm from the sediment (black dots) and just below the low water line (grey dots). Location IV (Oosterom; D,E) measured with fixed sensors at 50 cm from the sediment at 3 plots (see Fig. 2C,D for location of sensors). Grey shading indicates the time frame when (post) harvest activities were performed. FTU: formazin turbidity unit

tivation on 2 occasions. Turbidity values also showed a higher and variable pattern over the entire transect (T22); it could not be confirmed whether this was due to local hydrodynamics or to mussel culture activities. The fixed sensors (Fig. 5D,E) did not indicate enhanced values during the (post) harvest activities on 7 November.

### 3.3. Correlation of turbidity sensors and SPM

High-resolution sampling with the turbidity sensors (Turb) were correlated to *in situ* concentrations of SPM in the water column. Correlations for the fisheries campaign in spring were described by SPM = 8.0 Turb ($R^2$ = 0.77) and for the harvest campaigns in autumn by SPM = 2.1 Turb ($R^2$ = 0.89). High SDs, especially in the higher end of the calibration curves, indicated that the water column sampled was patchy and varied within a small spatial scale. Large variations were observed in results for both the water sampling (filters) and the turbidity sensors. This indicates that care should be taken with interpretation of the absolute concentrations of suspended material (in SPM); therefore, Figs. 3 to 5 are expressed in turbidity (FTU) rather than in SPM values and focus on the relative increases and decreases throughout transects. Excluding the high-variability samples (>100 mg $l^{-1}$ SPM; >40 FTU turbidity) improved the correlation coefficient ($R^2$ = 0.93), resulting in SPM = 2.5 Turb for the combination of fisheries and harvest samples. Using this conversion indicates that background values vary between 13 and 25 mg $l^{-1}$, and the highest values at Locations III and IV were estimated to range between 40 and 80 mg $l^{-1}$. As maximum values at Locations I and II exceeded turbidity values of 40 FTU, it is questionable if maximum values (>500 mg $l^{-1}$ and 200 mg $l^{-1}$, respectively) represent accurate estimates. The fraction of organic material was low (17 ± 5%, mean ± SD) for all samples, with lower values observed for samples collected within the sediment plumes.

### 3.4. Satellite data

In the spectral angle mapper, a tolerance of 0.0007 gave the best results; when the tolerance was set to lower than 0.0007, a smaller portion of the plumes was mapped, while increasing the tolerance over 0.0007 led to cloud shadows being mapped as plumes. Fig. 6A,B show the true colour image with and without mapped plumes. Individual plumes reach from 1 to over 5 km. Some plumes overlap, so that the longest plume (originating from 2 ships) is >8 km in length. Overlays per spectral band showed

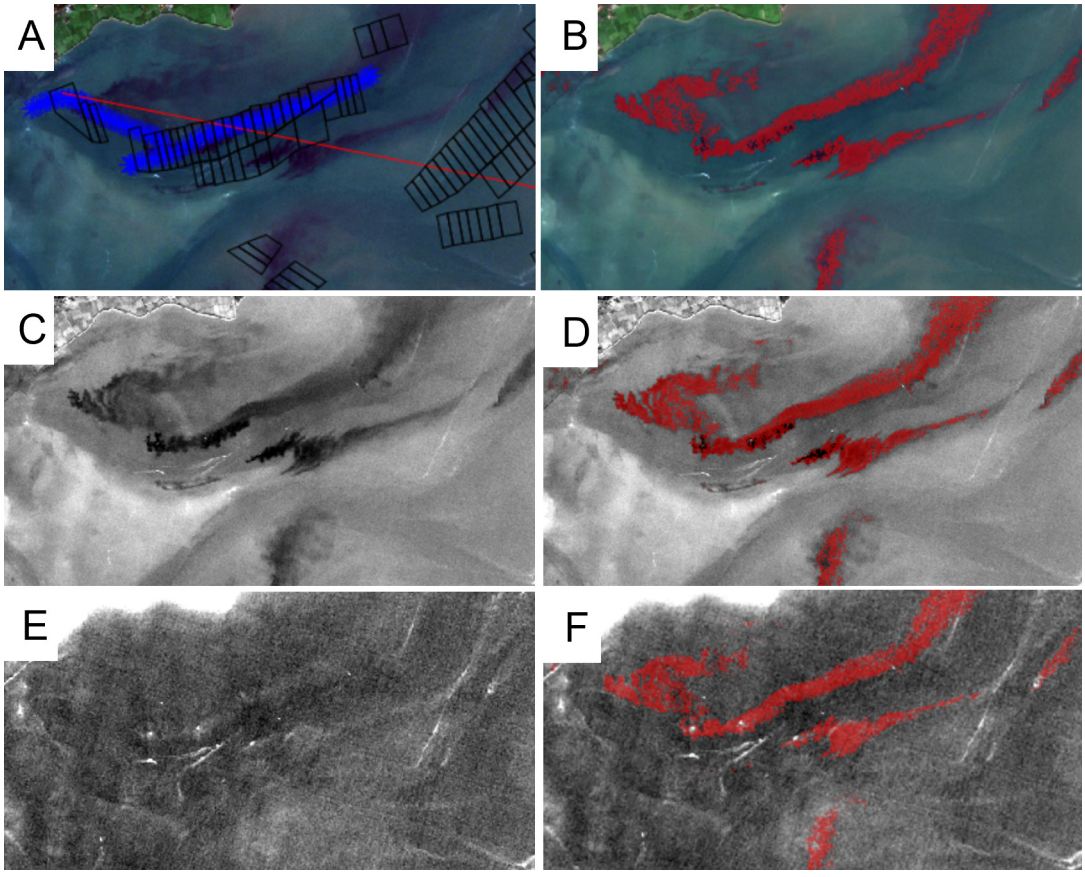


Fig. 6. (A) True colour composite of Sentinel-2, 7 November 2017, 10:52 h UTC, at location IV (Oosterom) in the Wadden Sea within the same timeframe when transects with towed turbidity meters were performed. The mussel cultivation plots are indicated by black polygons, the transect of the vessel is in blue (same as in Fig. 2D) and the transect used for image analysis is the red line. (B) True colour composite with the mapped plumes in red. (C,D) Sentinel-2 band 3 (560 nm) and (E,F) band 8a (865 nm) without (C,E) and with (D,F) the mapped plumes (in red)

that the plumes are clearly visible in the visible range (Fig. 6C,D) and cannot be distinguished from variability in the surroundings in the NIR (Fig. 6E,F).

From Fig. 6E,F (865 nm), which shows colouring from black (low reflection) to white (high reflection), it can be read that the small areas with a brighter colour due to higher SPM loads are found only where the ships are located; no plume shapes are visible. The other white lines in the image are also visible in Fig. 6A,B and seem to be caused by white caps due to shipping or waves at locations where different water masses meet.

Overlays with the transect confirmed the observation that the plumes are visible in the visual range but not specifically in the NIR (Fig. 7). Band 1 (ultra-blue) does show variability correlating with the plumes. Bands 2 (blue) and 3 (green) are the most influenced; bands 4 (red) and 5 (red to NIR) show only a slight effect, and all other bands (6–8a) show no correlation with the mapped plumes. This spectral analysis shows that the long dark plumes that are visible in the satellite image consist of CDOM instead of SPM. These CDOM molecules do not affect the NIR spectral bands like SPM does but instead absorb light in the visible range and turn the colour of the water dark.

A similar plot was made to check the black sediments criterion (Fig. 7B). The second criterion is met for the plume pixels: the maximum marine reflectance in 3 visible bands (2, 3 and 4) is low for a relatively high turbidity (maximum reflectance < 0.07). For some pixels around 400, the criterion is also (just) met, but these are not mapped as a plume. The first criterion, NIR marine reflectance is greater than a threshold for turbid waters, is also met: band 8a > 0.01, but this is the case for the whole area. However, band 8a is not additionally elevated in the detected plumes. This confirms that the SPM in the plumes is not elevated compared to the surroundings and therefore that the plumes are not black sediments but that, instead, the absorption in the visible range

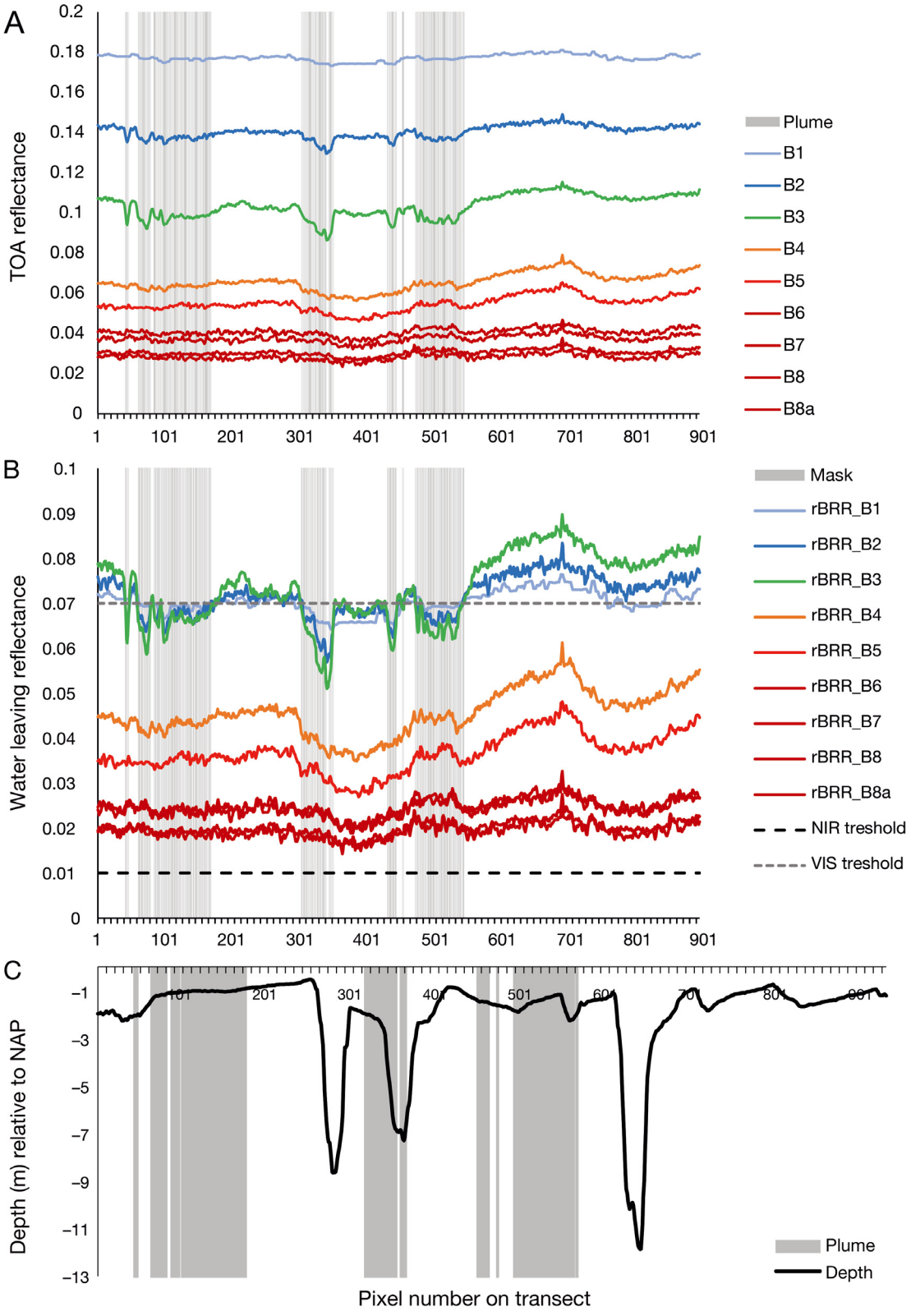


Fig. 7. (A) Top of the atmosphere (TOA) reflectance over the transect as shown in Fig. 6 (red line), with pixels numbered from northwest to southeast. The plume mask is indicated by the grey vertical lines. (B) A similar plot after Rayleigh correction (rBRR), including the thresholds from the black sediments approach. (C) Depth profile (in m, relative to NAP) for reference on the same transect. Note that depth varies in the area depending on the tide. B: band; NIR: near infrared; VIS: visible; NAP: Amsterdam Ordnance Datum, reference for sea level

is caused by CDOM. For reference, the depth profile has been added as Fig. 7C. There is no correlation between the (absence of) plumes and the depth.

To calculate the background reflection in band 3, the Rayleigh corrected values were averaged over the transect for those pixels that were not indicated as plumes. The average rBRR for these pixels was 0.081. For the pixel in the transect with the lowest reflection, this value was 0.05, meaning a reduction in reflection of 37%.

## 4. DISCUSSION

### 4.1. Spatio-temporal dynamics of sediment and dissolved organic matter plumes

This study demonstrated that mussel seed fisheries and harvest activities on cultivation plots in the Wadden Sea temporarily enhance turbidity in the water column. Measurements with towed sensors also indicated that impacts were local, which suggests that resuspended sediments settle quickly. Case studies presented in our study were expected to represent maximum impact as a result of fishing intensity, culture activity (post-harvest cleaning) and/or sediment characteristics (areas known for muddy and organic-rich sediments were selected). Given the large spatial and temporal differences in sediment characteristics, water quality and current velocity in the Wadden Sea (Hommersom et al. 2010), impacts are expected to vary considerably within the estuary. Results can therefore not be extrapolated to the scale of impact for the entire sector or at the ecosystem-scale. Yet assessment of maximum impacts helps to estimate to what extent this activity is a threat to the marine ecosystem (Halpern et al. 2007) and identifies if further in-depth studies defining cause–effect relationships are relevant for assessing ecosystem-wide effects. Furthermore, values presented here refer directly to commercial situations and thus provide empirical measurements that are often lacking.

Turbidity enhancement during seed fisheries was several-fold higher than that during harvest on culture plots, respectively up to a maximum of 16 to 40 and 4 to 6 times higher than background values. Given that during fisheries multiple boats are active at the same location, while harvest is performed with 1 vessel, this is likely the cumulative effect of higher fishing effort (Pastor et al. 2020). Turbidity naturally varies spatially and on short (tidal) and seasonal time scales (Hommersom et al. 2010). Comparing our data with a long-term monitoring program where SPM in the Wadden Sea is measured on a monthly basis (www.waterbase.nl) suggests that only the values observed at Location I during seed fisheries (>500 mg $l^{-1}$) exceeded natural variability in the Wadden Sea (up to 100–300 mg $l^{-1}$ for the different monitoring stations), whereas the other 3 case study locations lay within natural variability. However, taking into account that high SDs were observed in the higher end of the calibration curves and that the correlation between turbidity and suspended particles may fail at high concentrations (Reilly & Bellis 1978, Clifford et al. 1995) indicates that care should be taken with the absolute (maximum) turbidity estimates presented in this study. Moreover, the long-term monitoring program likely underestimates maximum values, as samples are not collected during heavy storms when high resuspension is expected but monitoring ships remain docked for safety reasons. Measurements with fixed sensors at the cultivation plots also highlighted that ambient turbidity varied on short temporal scales. Sediment was resuspended when the tides were turning, which resulted in turbidity values that almost doubled. For all case studies, towed sensors were deployed 1.5 m below the surface, indicating that at the fisheries locations, observations were obtained relatively close to the sea floor (Locations I and II), while at the culture plots (Locations III and IV), the upper water column was measured. Evaluation of turbidity across depth gradients (pilot studies) indicated that the highest turbidity could be expected in the upper layer and suggests that turbidity is to a great extent originating from water leaving the mussel vessel. It can however not be ruled out that values observed at Locations III and IV underestimated sediment resuspension, as the lower water column was not investigated.

Maximum turbidity values were observed in the middle of the fishery zones and right at the culture plots where activity took place. The turbidity values dropped back to background values in the vicinity of the fishery or harvest zone. Another indication of local turbidity enhancement was the patchiness of the sediment plume. The limited spatial magnitude of the sediment plume as observed by turbidity measurements in the field study was however not confirmed by the satellite image analysis, which identified a plume with a scale up to 5 km. Further spectral analysis of the satellite imagery showed that the plumes observed by satellite were caused by highly absorbing material (CDOM) instead of by suspended sediments. The reflection in Sentinel-2 band 3 is up to 37% lower than that in the surroundings, while in the infrared or NIR, no elevated reflection

was seen, indicating no elevated suspended sediment concentrations. Checking with the 2 criteria defined by Vanhellemont & Ruddick (2015) confirmed that the criteria for both the presence of absorbing substances (CDOM) and the presence of elevated sediment concentrations were met for the plumes. However, only the criterion for CDOM was different than that for its surroundings: the background values of the Wadden Sea also met the criterion for elevated sediment concentrations. CDOM is the coloured part of dissolved organic materials, which are a product of decaying material and include organic acids such as humic acid. In mussel beds, these materials can for example originate from mussel faecal pellets (Brocks et al. 1999). Turbidity measurements with sensors (such as Infinity used in the field study) rely on the amount of light scattered by particles in the water column (Sadar 2003), and the wavelengths applied in turbidity measurements are usually in the NIR range to eliminate the influence of any coloured substances. Colouration by CDOM will thus not be identified by these sensors. Along with turbidity, CDOM seems thus an important consideration for determining light attenuation in a water body within the dark water plume.

### 4.2. Comparison to other impact studies

Direct comparisons to other *in situ* case studies are difficult, as the magnitude of impact depends on sediment type and level of disturbance. Nevertheless, comparing our results to the few other field observations presented in literature indicates that the magnitude of the suspended sediment concentrations observed in our study (4- to 40-fold) was considerably higher compared to the 16% enhanced SPM values reported by Riemann & Hoffmann (1991) and comparable to the nearly 10-fold increase observed by Pastor et al. (2020) for a single mussel vessel performing a maximum of 12 (experimental) dredge events within an area of 3 ha in Limfjord, Denmark. As the commercial vessels in our case studies were fishing continuously, fisheries effort at locations I and II was higher, though the area covered was also >10-fold larger (Table 1). Furthermore, lighter dredges are used in Denmark, which reduces drag resistance, halves sediment retainment in the dredge and thus reduces resuspension of sediment at the surface (Frandsen et al. 2015). Large heterogeneity in sediment properties has been observed throughout the Wadden Sea (Dankers et al. 2006), and silt content differs per region (Fig. S1 in the Supplement at www.int-res.com/articles/suppl/q015p145_supp.pdf). These monitoring data indicate that the area surrounding Location III indeed consists of higher fractions of silt in comparison to the other locations in our study (Fig. S2), suggesting that sediments are more easily resuspended in the water column. This was however not confirmed by the field observations. Furthermore, the spatial extent of a plume is affected by settling velocity of resuspended material and the current speed at which the particles are transported. Higher flow velocities generally lead to more advection, resulting in higher water entrainment (dilution) in the plume and larger spatial distribution. Although flow velocities in the Wadden Sea can reach up to 1.5 m $s^{-1}$, during our field campaigns velocities up to 0.5 m $s^{-1}$ were predicted. These velocities are considerably higher compared to the Danish case study (up to 0.15 m $s^{-1}$), suggesting more dilution and larger distribution of the plume. Pastor et al. (2020) estimated a maximum impact range between 260 and 540 m for the mussel fisheries in the Limfjorden, but for most of the experimental fishing sessions, they predicted sediment plumes within 200 m from the fisheries activity. Their approach included empirical measurements with light loggers which were used for model calibration and validation. The use of light loggers suggests that both suspended particles and colouration of the water column (by e.g. CDOM) were evaluated, though the model was based on suspended particles. Their results confirm our field observations that the spatial extent of the (resuspended particle) plume is restricted to the local vicinity of the fisheries zone. Furthermore, the patchiness observed within our plumes together with data from the fixed sensors indicates quick settlement of particles. Similar patterns were observed for mussel fisheries in Denmark, which indicated that suspended sediments settled within 30 min (Riemann & Hoffmann 1991), and were confirmed by Pastor et al. (2020), who demonstrated that larger sand particles sank within the first 10 min after the resuspension event and that silt particles could be suspended up to 1 h. Measurements taken while dredging for oyster shells (James River estuary, Virginia, USA) also demonstrated that the sediment plume settled within an hour (Battisto & Friedrichs 2003).

Furthermore, very few empiric measurements are available for sediment disturbance by other anthropogenic activities in the Wadden Sea, such as demersal fisheries and dredging in harbours and shipping routes. Data from other study areas, however, suggest that magnitude and spatial scale of the dredging

plume is considerably larger than that measured for mussel fisheries in our study (Kirby & Land 1991, Pennekamp et al. 1996,Clarke et al. 2007). Van Duren et al. (2015) simulated sediment transport by various anthropogenic sources and concluded that particularly dredging and to a lesser extent demersal shrimp fisheries contribute to sediment transport in the Wadden Sea. Mussel fisheries and harvest on plots were ranked lowest in terms of sediment transport.

### 4.3. Conclusions

Our study showed that the suspended sediment concentration is enhanced during mussel fisheries and aquaculture activities in the Wadden Sea but that the effects are limited in time and space. As we presented case studies that were expected to represent the maximum impact of commercial activities, we conclude that there is no specific need for further in-depth studies that allow upscaling to ecosystem-wide effects. Furthermore, the mussel sector is in transition, aiming for the collection of mussel seed from suspended cultures, and fisheries on seeds beds are gradually being phased out in the Wadden Sea (Kamermans & Capelle 2019). Sediment resuspension will therefore in the near future be limited to activities on cultivation plots, which in our study was identified to result in lower turbidity enhancement compared to fisheries. Finally, our study has shown that along with turbidity, it is of interest to determine CDOM when evaluating the scale of the dark water plume created by mussel cultivation activities.

*Acknowledgements*. The field study was part of the national KOMPRO research program financed by the Dutch Mussel Growers Association (PO Mosselcultuur), and we thank the steering committee for valuable discussions. The Ministry of Economic Affairs provided access to the vessels 'Phoca' and 'Asterias', and support of the crew during the sampling campaigns was invaluable. We specially thank the mussel farmers who provided access to their cultivation plots and all mussel farmers for their patience during the seed fisheries campaigns. Finally, we thank Hans Verdaat for field assistance and Beatriz Ortiz (student from the HZ University of Applied Sciences) for her help throughout the study. The field measurements described in the current publication were based on the non-peer-reviewed research report Jansen & Capelle (2018), available at: https://doi.org/10.18174/454788. The satellite image analysis was carried out within the CoastObs project, which received funding from the European Union's Horizon 2020 research and innovation program (grant agreement no. 776348).

LITERATURE CITED

Airoldi L, Beck MW (2007) Loss, status and trends for coastal marine habitats of Europe. Oceanogr Mar Biol Annu Rev 45:345–405

Austen I, Andersen TJ, Edelvang K (1999) The influence of benthic diatoms and invertebrates on the erodibility of an intertidal mudflat, the Danish Wadden Sea. Estuar Coast Shelf Sci 49:99–111

Battisto GM, Friedrichs CT (2003) Monitoring suspended sediment plume formed during dredging using ADCP, OBS and bottle samples. Proc Coast Sediments 2003, Clearwater Beach, FL

Beukema JJ, Cadée GC (1996) Consequences of the sudden removal of nearly all mussels and cockles from the Dutch Wadden Sea. Mar Ecol 17:279–289

Brockmann C, Doerffer R, Peters M, Stelzer K, Embacher S, Ruescas A (2016) Evolution of the C2RCC neural network for Sentinel 2 and 3 for the retrieval of ocean colour products in normal and extreme optically complex waters. In: Ouwehand L (ed) Proc Living Planet Symp 740:54

Brocks P, Rohjans D, Scholz-Böttcher BM, Rullkötter J (1999) Molecular composition of organic matter in the sediment of a mussel bee as an indicator of ecological variations. Senckenb Marit 29:45–50

Cadée GC, Hegeman J (1974) Primary production of the benthic microflora living on tidal flats in the Dutch Wadden Sea. Neth J Sea Res 8:260–291

Castorani MC, Glud RN, Hasler-Sheetal H, Holmer M (2015) Light indirectly mediates bivalve habitat modification and impacts on seagrass. J Exp Mar Biol Ecol 472:41–53

Clarke D, Reine K, Dickerson C, Zappala S, Pinzon R, Gallo J (2007) Suspended sediment plumes associated with navigation dredging in the Arthur Kill waterway, New Jersey. Proc 18th World Dredging Congress 2007: 1135–1154

Clifford N, Richards K, Brown R, Lane S (1995) Laboratory and field assessment of an infrared turbidity probe and its response to particle size and variation in suspended sediment concentration. Hydrol Sci J 40:771–791

Craeymeersch JA, van Stralen MR, Smaal AC (2023) Impact of mussel seed fishery on subtidal sediment and macrozoobenthos in the western Wadden Sea. J Sea Res 192: 102353

Cranford PJ (2019) Magnitude and extent of water clarification services provided by bivalve suspension feeding. In: Smaal A, Ferreira J, Grant J, Petersen J, Strand Ø (eds) Goods and services of marine bivalves. Springer, Cham

Dankers N, Koelemaij K (1989) Variations in the mussel population of the Dutch Wadden Sea in relation to monitoring of other ecological parameters. Helgol Meeresunters 43:529–535

Dankers N, Cremer J, Dijkman E, Brasseur S and others (2006) Ecologische atlas Waddenzee. https://www.waddenzee.nl/fileadmin/content/Bestuur/pdf/ecologische_atlas.pdf

De Groot A, Brinkman B, Fey F, van Sluis C and others (2013) Biobouwers als onderdeel van een kansrijke waterveiligheidsstrategie voor Deltaprogramma Waddengebied. IMARES-rapport C163/13A. https://edepot.wur.nl/280407

De Jonge VN (1992) Physical processes and dynamics of microphytobenthos in the Ems estuary (The Netherlands). PhD thesis, State Universiteit Groningen

Dolmer P, Kristensen PS, Hoffmann E (1999) Dredging of blue mussels (*Mytilus edulis* L.) in a Danish sound: stock

sizes and fishery-effects on mussel population dynamic. Fish Res 40:73–80

Dolmer P, Kristensen T, Christiansen ML, Petersen MF, Kristensen PS, Hoffmann E (2001) Short-term impact of blue mussel dredging (*Mytilus edulis* L.) on a benthic community. Hydrobiologia 465:115–127

Dolmer P, Christensen HT, Hansen BW, Vismann B (2012) Area-intensive bottom culture of blue mussels *Mytilus edulis* in a micro-tidal estuary. Aquacult Environ Interact 3:81–91

Duarte CM (2002) The future of seagrass meadows. Environ Conserv 29:192–206

Elias EPL, Stive MJF, Roelvink JA (2005) Impact of back-barrier changes on ebb-tidal delta evolution. J Coast Res 21:460–476

Elias EPL, Van Der Spek AJF, Wang ZB, De Ronde J (2012) Morphodynamic development and sediment budget of the Dutch Wadden Sea over the last century. Geol Mijnb 91:293–310

Figueiredo BRS, Mormul RP, Chapman BB, Lolis LA, Fiori LF, Benedito E (2016) Turbidity amplifies the non-lethal effects of predation and affects the foraging success of characid fish shoals. Freshw Biol 61:293–300

Frandsen RP, Eigaard OR, Poulsen LK, Tørring D, Stage B, Lisbjerg D (2015) Reducing the impact of blue mussel (*Mytilus edulis*) dredging on the ecosystem in shallow water soft bottom areas. Aquatic Conserv: Mar Freshw Ecosyst 25:162–173

Giesen WBJT, van Katwijk MM, den Hartog C (1990) Eelgrass condition and turbidity in the Dutch Wadden Sea. Aquat Bot 37:71–85

Grasshoff K, Kremling K, Ehrhardt MG (1999) Methods of seawater analysis, 3rd edn. Wiley-VCH, Weinheim

Halpern BS, Selkoe KA, Micheli F, Kappel CV (2007) Evaluating and ranking the vulnerability of global marine ecosystems to anthropogenic threats. Conserv Biol 2:1301–1315

Hawkins AJS, Smith RFM, Bayne BL, Héral M (1996) Novel observations underlying fast growth of suspension-feeding shellfish in turbid environments: *Mytilus edulis.* Mar Ecol Prog Ser 131:179–190

Henley WF, Patterson MA, Neves RJ, Lemly AD (2000) Effects of sedimentation and turbidity on lotic food webs: a concise review for natural resource managers. Ref Fish Sci 8:125–139

Hommersom A, Wernand MR, Peters S, de Boer J (2010) A review on substances and processes relevant for optical remote sensing of extremely turbid marine areas, with a focus on the Wadden Sea. Helgol Mar Res 64:75–92

Jafar-Sidik M, Gohin F, Bowers D, Howarth J, Hulle T (2017) The relationship between suspended particulate matter and turbidity at a mooring station in a coastal environment: consequences for satellite-derived products. Oceanologia 59:365–378

Kaiser MJ, Clarke KR, Hinz H, Austen MCV, Somerfield PJ, Karakassis I (2006) Global analysis of response and recovery of benthic biota to fishing. Mar Ecol Prog Ser 311:1–14

Kamermans P, Capelle J (2019) Provisioning of mussel seed and its efficient use in culture. In: Smaal A, Ferreira J, Grant J, Petersen J, Strand Ø (eds) Goods and services of marine bivalves. Springer, Cham, p 27–49

Kirby R, Land JM (1991) The impact of dredging: a comparison of natural and man-made disturbances to cohesive sedimentary regimes. Paper B3, Proc CEDA-PIANC Conf, 13–14 Nov 1991, Amsterdam

Lotze HK (2007) Rise and fall of fishing and marine resource use in the Wadden Sea, southern North Sea. Fish Res 87: 208–218

McBride RA, Anderson JB, Buynevich IV, Cleary W and others (2013) Morphodynamics of barrier systems: a synthesis. In: Shroder JF (ed) Treatise on geomorphology, Vol 10. Academic Press, San Diego, CA, p 166–244

McLeod IM, Parsons DM, Morrison MA, Le Port A, Taylor RB (2012) Factors affecting the recovery of soft-sediment mussel reefs in the Firth of Thames, New Zealand. Mar Freshw Res 63:78–83

Morrison MA, Lowe ML, Parsons DM, Usmar NR, McLeod IM (2009) A review of land-based effects on coastal fisheries and supporting biodiversity in New Zealand. Ministry of Fisheries, Wellington

Nieuwaal M (2001) Requirements for sediment plumes caused by dredging. MSc thesis, Delft University of Technology. https://repository.tudelft.nl/islandora/object/uuid:56fc873f-d6a8-4f69-980a-73ffadff24b2/datastream/OBJ/download

Ortega JCG, Figueiredo BRS, da Gracia WJ, Agostinho AA, Bini LM (2020) Negative effect of turbidity on prey capture for both visual and non-visual aquatic predators. J Anim Ecol 89:2427–2439

Österling ME, Arvidsson BL, Greenberg LA (2010) Habitat degradation and the decline of the threatened mussel *Margaritifera margaritifera*: influence of turbidity and sedimentation on the mussel and its host. J Appl Ecol 47: 759–768

Pastor A, Larsen J, Mohm C, Saurel C, Petersen JK, Maar M (2020) Sediment transport model quantifies plume length and light conditions from mussel dredging. Front Mar Sci 7:576530

Pennekamp JGS, Epskamp RJC, Rosenbrand WF, Mulli A, Wessel GL, Arts T, Deibel IK (1996) Turbidity caused by dredging; viewed in perspective. Terra et Aqua 64: 10–17

Philippart CJM, Salama MS, Kromkamp JC, van der Woerd H, Zuur AF, Cadée GC (2013) Four decades of variability in turbidity in the western Wadden Sea as derived from corrected Secchi disk readings. J Sea Res 82:67–79

Reilly FJ, Bellis V (1978) A study of the ecological impact of beach nourishment with dredged materials on the intertidal zone. Inst Coast Mar Res Tech Rep 4

Riemann B, Hoffmann E (1991) Ecological consequences of dredging and bottom trawling in the Limfjord, Denmark. Mar Ecol Prog Ser 69:171–178

Ruescas A, Müller D (2021) S3TBX Rayleigh correction tutorial. Brockmann Consult and ESA. https://step.esa.int/docs/tutorials/S3TBX_Rayleigh_Correction_Tutorial.pdf

Sadar M (2003) Turbidity measurement: a simple, effective indicator of water quality change. Hach Hydromet 182. https://www.ott.com/download/whitepaper-turbidity-measurements/

Schröder T, Stank J, Schernewski G, Krost P (2014) The impact of a mussel farm on water transparency in the Kiel Fjord. Ocean Coast Manage 101:42–52

Smaal AC, Craeymeersch JA, van Stralen M (2021) The impact of mussel seed fishery on the dynamics of wild subtidal mussel beds in the western Wadden Sea. Neth J Sea Res 167:101978

Thrush S, Hewitt J, Cummings V, Ellis J, Hatton C, Lohrer A, Norkko A (2004) Muddy waters: elevating sediment input

to coastal and estuarine habitats. Front Ecol Environ 2: 299–306

Troost K, van der Meer J, Stralen M (2022) The longevity of subtidal mussel beds in the Dutch Wadden Sea. J Sea Res 181:102174

Van Duren LA, van Kessel T, Brinkman AG, de Kluijver A, Fey F, Schmidt CA (2015) Verkenning Slibhuishouding Waddenzee. Deltares rapport. http://publications.deltares.nl/WeL1818.pdf

Vanhellemont Q, Ruddick K (2015) Advantages of high quality SWIR bands for ocean colour processing: examples from Landsat-8. Remote Sens Environ 161:89–106

Vroom J, Elias EPL, Lescinski J, Wang ZB (2012) Assessment of the effects of the Zuider Sea closure on the hydrodynamics of the Wadden Sea inlets. Coast Eng Proc 1: management.47

Warren MA, Simis SGH, Martinez-Vicente V, Poser K and others (2019) Assessment of atmospheric correction algorithms for the Sentinel-2A MultiSpectral Imager over coastal and inland waters. Remote Sens Environ 225:267–289

*Editorial responsibility: Jonathan Grant, Halifax, Nova Scotia, Canada*
*Reviewed by: L. A. van Duren and 2 anonymous referees*

*Submitted: October 7, 2022*
*Accepted: March 21, 2023*
*Proofs received from author(s): May 23, 2023*